

Molecular Cloning, Pharmacological Characterization, and Brain Mapping of the Melanocortin 4 Receptor in the Goldfish: Involvement in the Control of Food Intake

JOSÉ MIGUEL CERDÁ-REVERTER, ANETA RINGHOLM, HELGI BIRGIR SCHIÖTH, AND RICHARD ECTOR PETER

Department of Biological Sciences (J.M.C.-R., R.E.P.), University of Alberta, Edmonton, Alberta, T6G 2E9 Canada; and Department of Neuroscience (A.R., H.B.S.), Unit of Pharmacology, Uppsala University, SE 751 24 Uppsala, Sweden

We report cloning, pharmacological characterization, tissue distribution, detailed brain mapping, and role in control of food intake of melanocortin 4 receptor in goldfish (gMC4R). The gMC4R protein has 68% identity with the human ortholog and is conserved in important functional domains. Pharmacological profiling showed similar affinities and potency order to hMC4R for MSH peptides, whereas MTII and HS024 were identified as high-affinity agonist and antagonist analogs, respectively. The gMC4R-mRNA was found in brain and some peripheral tissues including the ovary, gill, and spleen. Detailed MC4R-mRNA mapping showed expression in main neuroendocrine and food intake-controlling areas. High expression levels were found in the telencephalon, preoptic

area, ventral thalamus, tuberal hypothalamus, and hypothalamic inferior lobe. By RT-PCR, low levels were also detected in the cerebellum, medulla, and spinal cord. Intracerebroventricular MTII administration inhibited food intake in 24-h fasted animals in a dose-dependent manner, whereas HS024 stimulated food intake in fed animals, suggesting that melanocortins exert a tonic inhibitory effect on food intake, which is mediated through central MC4R signaling. The conserved central expression pattern and physiological role in regulation of food intake for the MC4R suggests that neuronal pathways of the melanocortin system may be important for regulation of energy homeostasis in most vertebrates. (*Endocrinology* 144: 2336–2349, 2003)

THE CONTROL OF energy homeostasis involves multifaceted interplay among diverse hypothalamic neuronal systems in addition to their interaction with reporter systems that convey peripheral energetic information to the central neuronal systems (1). Recent evidence has demonstrated that the central melanocortin system is a nodal point in the control of energy balance in mammals (2). Melanocortins are produced by posttranscriptional processing of proopiomelanocortin (POMC) precursor and are mainly comprised of ACTH and α -, β -, and γ -melanocyte-stimulating hormones (MSH; Ref. 3). Two discrete groups of neurons in the arcuate nucleus of hypothalamus and the caudal region of the nucleus of the tractus solitarius of the medulla produce POMC (4) that is mainly processed to α -MSH and β -endorphin (3).

Melanocortin signaling is mediated by binding to a family of specific G protein-coupled receptors that positively couple to adenylyl cyclase. Five melanocortin receptors (MCRs), MC1R–MC5R, have been characterized by molecular cloning in tetrapods, but only MC3R and MC4R are abundantly

expressed within the mammalian the central nervous system (CNS). Subtype 2 receptor binds ACTH, whereas the four other MCRs distinctively recognize MSHs (5, 6). Atypically, melanocortin signaling is not exclusively regulated by binding of endogenous agonists because naturally occurring antagonists, agouti and agouti-related protein (AGRP), compete with melanocortin peptides by binding to MCRs (7–9). Agouti protein is a potent melanocortin antagonist at MC1R and MC4R and relatively weak at MC3R. In mice, agouti is exclusively produced within the hair follicle, and it locally regulates the production of pigment in follicular melanocytes by antagonizing the effects of α -MSH on MC1R (10). In contrast, AGRP is mainly produced within the hypothalamic arcuate nucleus and the adrenal gland, and it is potent in inhibiting melanocortin signaling at MC3R and MC4R but is not active at MC1R (11).

Central activation of MC3R and MC4R is thought to mediate melanocortin effects on energy balance (7) because both MC3R knockout rat (12) and MC4R knockout mice (13) display severe alterations in energy homeostasis. Interruption of α -MSH central signaling by ubiquitous constitutive expression of agouti gene in obese yellow mice (A^y) results in hyperphagia, hyperinsulinemia, increased linear growth, maturity-onset obesity, and yellow fur (10). A similar metabolic syndrome is also observed in transgenic mice ubiquitously overexpressing agouti or AGRP genes (11, 14) and in the MC4R knockout mice (13). However, mice with multiple copies of the agouti gene expressed under the control of a skin-specific promoter do not exhibit the obesity-related phenotype but manifest yellow fur (15). This suggests that antagonizing of central α -MSH signaling by agouti protein in

Abbreviations: AGRP, Agouti-related protein; CNS, central nervous system; dCTP, deoxycytidine triphosphate; DTT, dithiothreitol; ECL, extracellular; HEK, human embryonic kidney; ICL, intracellular; icv, intracerebroventricular; MCR, melanocortin receptor; MSH, melanocyte-stimulating hormone; NAPv, anterior periventricular nucleus; NDP-MSH, [125 I][Nle 4 , d-Phe 7] α -MSH; NLTp, posterior part of the lateral tuberal nucleus; NPO, preoptic nucleus; NPP, periventricular part of the preoptic nucleus; NPY, neuropeptide Y; PAF, paraformaldehyde; PB, phosphate buffer; PBSSK, pBluescript II SK vector; POMC, proopiomelanocortin; SSC, standard saline citrate buffer; SSPE, sodium chloride/sodium phosphate/EDTA; 35 S-UTP, 35 S-uridine 5-triphosphate; TMD, transmembrane domain.

obese yellow mice is responsible for this metabolic syndrome. Accordingly, central administration of the C-terminal fragment of AGRP (16) or chemical antagonists for MC3R and MC4R increase food intake in rodents (17, 18), and intracerebroventricular (icv) injections of the melanocortin receptor agonist, MTII, produces a dose-dependent reduction in food intake in mice (17). However, MC4R-deficient mice do not respond to anorectic effects of MTII, suggesting that α -MSH inhibits feeding primarily by activating MC4R (19).

In contrast to the increasing understanding of the central mechanisms for regulation of food intake and metabolism in mammals (1), little is known about the central regulation of energy homeostasis in nonmammalian vertebrates. Studies in fish have demonstrated that these molecular mechanisms and central neuronal pathways could be determined early in the evolution. Central neuronal systems such as cholecystokinin, bombesin, orexins, cocaine- and amphetamine-induced transcript, neuropeptide Y (NPY), galanin, and corticotrophin-releasing hormone have been shown to be involved in the control of food intake in goldfish (20). Structural conservation of α -MSH during vertebrate evolution suggests preserved functions throughout the evolutionary process. Previous results have provided the first demonstration of melanocortin receptors in fish (21). However, involvement of the melanocortin system in energy homeostasis in ectothermic species remains unexplored. We first approached this question by molecular cloning and pharmacological characterization of goldfish MC4R. We next mapped the MC4R-mRNA production in the goldfish brain. Finally, agonist and antagonist ligands were icv administered to study the role of melanocortin in food intake. The results provide the first brain mapping of melanocortin receptors in a species other than rat; the first identification of effective melanocortin agonist and antagonist ligands for studies in fish and, for the first time, demonstrate a role for the central melanocortin system in the control of food intake in an ectothermic species.

Materials and Methods

Animals and reagents

Male and female goldfish were purchased from Mount Parnell Fisheries (Mercersburg, PA). Fish were acclimated to a constant photoperiod of 16-h light/8-h darkness in 65-liter tanks receiving a constant flow of aerated water at 20 C for at least 1 wk before experimentation. Fish were fed at 2% wet body weight ration once a day with trout pellets (Moore Clark, St. Andrews, New Brunswick, Canada). Animals were anesthetized in 0.02% tricaine methanesulfonate (MS-222, Syndel Laboratories Vancouver, British Columbia, Canada) for 2 min before icv injection, perfusion, or decapitation for tissue collection. All experiments were carried out in accordance with the principles published in the Canadian Council on Animal Care's guide to the care and use of experimental animals. Unless otherwise indicated, all reagents were purchased from Sigma (St. Louis MO).

Molecular cloning and DNA sequencing

Filters from a goldfish genomic library made in the vector λ -GEM-11 (22), kindly provided by Dr. K. L. Yu (Department of Zoology, University of Hong Kong, Hong Kong), containing approximately 10^6 clones were screened with a zebrafish MC4R probe consisting of full coding sequence (GenBank accession no. AY078989). Probe was labeled with deoxycytidine triphosphate (dCTP) [α - 32 P] (Amersham Biosciences, Piscataway, NJ) using the random primer labeling kit (Invitrogen, Carlsbad,

CA). Membranes were prehybridized for at least 3 h in hybridization solution [40% formamide, 6 \times sodium chloride/sodium phosphate/EDTA (SSPE), 0.5% sodium dodecyl sulfate, 5 \times Denhardt's solution, and 10 μ g/ml yeast tRNA type III (1 \times SSPE contains 150 mM NaCl; 1 mM EDTA; 9 mM NaH₂PO₄; pH 7.4)]. Hybridization was carried out overnight in fresh hybridization solution containing 10^6 cpm/ml dCTP [α - 32 P] at 42 C. Final washes were performed in 1 \times SSPE at 42 C. After 4 d of exposure to autoradiographic films, seven clones (clone nos. 721, 1541, 1551, 631, 931, 1641, 13111) were subjected to two additional purification rounds. Fragments were released by digestion with Sac I (Promega Corp., Madison, WI) and subcloned into pBluescript II SK vector (PBSSK; Stratagene, La Jolla, CA). Following restriction mapping and Southern blot analysis, clones 931 and 1641 were selected for subsequence characterization.

A *Pst*I fragment of 2820 bp from clone 931 was subcloned into PBSSK and sequenced. The latter fragment was found to contain an open reading frame of 197 amino acids including the motif ASIWSSLAIAVDRYITI in good consensus with the class A of rodopsin-like G protein-coupled receptor (23). Because 931-*Pst*I fragment was truncated at its 5' end, specific primers for upstream sequencing of the original clone 931 were designed. Sequencing went on as far as finding the first upstream stop codon in frame with a DRY motif. New specific primers were then designed for sequencing downstream and thus sequence confirmation.

Similarly, the clone 1641 subcloned into PBSSK was double digested with *Eco*RI and *Bam*HI (Invitrogen) and a 6-kb fragment was again subcloned into PBSSK. A digestion with *Xho*I (Invitrogen) of the latter construct was finally used to generate a 2.9-kb fragment that was subcloned into the same plasmid vector, named 1641-*Xho*I-8, and sequenced. Inserts were sequenced on both strands by means of automated sequencer 373A (PE Applied Biosystems, Foster City, CA) according to the manufacturer's protocol. Sequences were compiled in a GenTool software package (BioTools Inc., Edmonton, CA) and compared with known MCR sequences from the National Center for Biotechnology Information database by using BlastX. Sequence alignments were performed using Pileup from the GCG package and ClustalX 1.81 from Canadian Bioinformatics Resources (<http://www.cbr.nrc.ca>). The nucleotide sequence of goldfish MC4R has been deposited with European Molecular Biology Laboratory Nucleotide Sequence Database under accession no. AJ534337.

Cloning in an expression vector and cell transfection

The entire coding region of the receptor sequence was amplified by touchdown PCR using Vent DNA polymerase (New England Biolabs Inc., Beverly, MA) and genomic clone 931 as template. Specific primers containing *Hind*III (HiMC4) and *Xho*I (XhMC4) restriction sites were used under the following conditions: 5 min at 95 C for one cycle, then 45 sec at 95 C, 30 sec at 56–54 C decreasing 0.5 C for 4 cycles and 30 sec at 72 C, and then 45 sec at 95 C, 30 sec at 58 C and 30 sec at 72 C for 26 cycles followed by a final cycle at 72 C for 10 min (0.2 mM dNTP, 0.4 μ M HiMC4 and XhMC4 primers, 1 \times Taq DNA polymerase buffer, 1.5 mM MgCl₂ and 0.5 U Taq DNA polymerase). The 5' primer (HiMC4) was a 24-mer with the sequence 5' AAG CTT ATG AAC ACC TCA CAT CAC 3'. The 3' primer (XhMC4) had the sequence 5' CTC GAG TCA TAC ACA CAG AGA CGC 3'. PCR fragments were isolated from low-melting-point gel, double digested with *Hind*III and *Xho*I restriction enzymes (Invitrogen), and then ligated into a modified pCEP4 expression vector (24). The new constructs were sequenced and found to be identical with the genomic clone. Human embryonic kidney (HEK) 293-EBNA cells were transiently transfected with the constructs using FuGENE transfection reagent (Boehringer Mannheim, Mannheim, Germany) diluted in OptiMEM medium (Invitrogen) according to the manufacturer's recommendations. The cells were grown in DMEM/Nut Mix F-12 with 10% fetal calf serum (Invitrogen) containing 0.2 mM L-glutamine (Invitrogen) and 250 μ g/ml G-418 (Invitrogen) and penicillin-streptomycin (100 U penicillin, 100 μ g streptomycin/ml; Invitrogen).

Radioligand binding and cAMP assay

Intact transfected cells were resuspended in 25 mM HEPES buffer (pH 7.4) containing 2.5 mM CaCl₂, 1 mM MgCl₂, and 2 g/liter bacitracin. Saturation experiments were performed in a final volume of 100 μ l for 3 h at 37 C and carried out with serial dilutions of [125 I][Nle⁴, D-Phe⁷]- α -

MSH (NDP-MSH). Nonspecific binding was defined as the amount of radioactivity remaining bound to the intact cells after incubation in the presence of 2000 nM unlabeled NDP-MSH. Competition experiments were performed in a final volume of 100 μ l. The cells were incubated in the well plates for 3 h at 37 C with 50 μ l binding buffer in each well containing a constant concentration of [¹²⁵I] NDP-MSH and appropriate concentrations of competing unlabeled ligands NDP-MSH, α -, β -, γ -MSH, MTII, or HS024. The incubations were terminated by filtration through glass fiber filters, Filtermat A (Wallac, Inc. Oy, Turku, Finland), which had been presoaked in 0.3% polyethylenimine, using a TOMTEC Mach III cell harvester (Orange, CT). The filters were washed with 5.0 ml of 50 mM Tris (pH 7.4) at 4 C and dried at 60 C. The dried filters were then treated with MeltiLex A (Perkin-Elmer, Wellesley, MA) melt-on scintillator sheets and counted with a 1450 microbeta counter (Wallac, Inc.). The results were analyzed with a software package suitable for radioligand-binding data analysis (Prism 3.0, GraphPad Software, Inc., San Diego, CA). Data were analyzed by fitting to formulae derived from the law of mass action by the method generally referred to as computer modeling. The binding assays were performed in duplicate wells and repeated three times. Nontransfected HEK293-EBNA cells did not show any specific binding for [¹²⁵I]NDP-MSH. NDP-MSH was radiiodinated by the chloramine T method and purified by HPLC. NDP-MSH; α -, β -, γ -MSH; MTII; or HS024 were purchased from Neosystem (Strasbourg, France).

cAMP was assayed on transfected HEK293-EBNA cells treated for 20 min at 37 C with 0.5 mM isobutylmethylxanthine. Cells were incubated with various concentrations of HS024 and MTII alone or with a fixed concentration (0.1 μ M) of HS024 for 30 min and then lysed by treatment with 0.4 M perchloric acid and neutralized with 5 M KOH. Then 25 μ l of the neutralized cAMP extract was added to a 96-well microtiter plate. The content of cAMP was then estimated (essentially according to Ref. 25) by adding to each well [³H]cAMP (0.14 pmol, ~11,000 cpm, specific activity 54 Ci/mmol; Amersham) and bovine adrenal binding protein and incubating at 4 C overnight. The incubates were thereafter harvested by filtration through glass fiber filters, Filtermat A (Wallac, Inc.), which had been presoaked in 0.3% polyethylenimine, using a TOMTEC Mach III cell harvester. Each filter was rinsed with 3 ml 50 mM Tris/HCl (pH 7.4) at 4 C and dried at 60 C. The dried filters were then treated with MeltiLex A melt-on scintillator sheets (Perkin-Elmer) and counted with 1450 Microbeta counter (Wallac, Inc.). The cAMP assays were performed in duplicate wells and repeated three times. Untransfected HEK293-EBNA cells showed no response to cAMP (data not shown).

RT-PCR and Southern blot analysis

Total RNA was purified from fresh tissues [testis, ovary, intestine, fat, liver, muscle, spleen, kidney, gill, dorsal skin, ventral skin, retina, heart, pituitary, and brain (olfactory bulb, telencephalon-preoptic area, hypothalamus, thalamus-optic tectum, cerebellum, medulla, and spinal cord)] and treated with RQ1-deoxyribonuclease (Promega Corp.). Superscript II reverse transcriptase (Invitrogen) was used for cDNA synthesis by priming with oligo (deoxythymidine)_{12–18} (Invitrogen). The cDNA was subsequently used as template for touchdown PCR with Taq DNA polymerase (Invitrogen) and specific primers designed within N- and C-terminal regions of the goldfish MC4R, respectively (Fig. 1). The following conditions were used: 5 min at 95 C for one cycle and then 45 sec at 95 C, 30 sec at 60–58 C decreasing 0.5 C for 4 cycles, and 45 sec at 72 C and then 45 sec at 95 C, 30 sec at 58 C, and 45 sec at 72 C for 31 cycles followed by a final cycle at 72 C for 10 min (0.2 mM dNTP, 0.4 μ M MC4-DTC-F and MC4-DTC-R primers, 1 \times Taq DNA polymerase buffer, 1.5 mM MgCl₂, and 0.5 U Taq DNA polymerase). The 5' primer (MC4-DTC-F) was a 19-mer with the sequence 5' TGG ACC GCA TCA TTC ATA C 3'. The 3' primer (MC4-DTC-R) had the sequence 5' ACG CCA GTC CAT ACC AG 3'. Subsequently PCR fragments were separated onto 1.2% agarose gel and transferred by capillarity to Hybond-N nylon

membrane (Amersham). Membranes were prehybridized for at least 3 h in hybridization solution [50% formamide, 6 \times SSPE, 0.5% sodium dodecyl sulfate, 5 \times Denhardt's solution, and 10 mg/ml yeast tRNA type III (1 \times SSPE contains 150 mM NaCl; 1 mM EDTA; 9 mM NaH₂PO₄; pH 7.4)]. Goldfish MC4R probe containing only the full coding region was labeled as before. Hybridization was carried out overnight in fresh hybridization solution containing 10⁶ cpm/ml dCTP [α -³²P] at 42 C. Final washes were performed in 0.1 \times SSPE at 65 C. Hybridization signals were scanned using PhosphorImager (Molecular Dynamics, Inc., Sunnyvale, CA) and ImageQuant software (Molecular Dynamics, Inc.).

As internal control of the reverse transcription (RT) step, touchdown PCR for β -actin cDNA amplification was also carried out under the following conditions: 5 min at 95 C for one cycle and then 45 sec at 95 C, 30 sec at 60–55 C decreasing 0.5 C for 10 cycles, and 30 sec at 72 C and then 45 sec at 95 C, 30 sec at 55 C, and 45 sec at 72 C for 25 cycles followed by a final cycle at 72 C for 10 min (0.2 mM dNTP, 0.4 μ M β -actin 1 and β -actin 2, 1 \times Taq DNA polymerase buffer, 1.5 mM MgCl₂, and 0.5 U Taq DNA polymerase). The primer sequences were 5' CTA CTG GTA TTG TGA TGG ACT CCG 3' and 5' TCC AGA CAG AGT ATT TGC GCT CAG 3' for β -actin 1 and β -actin 2, respectively (26).

In situ hybridization

In situ hybridization experiments were carried out as described previously (27). Animals were anesthetized and then transcardially perfused with 20 ml physiological saline solution (NaCl 0.65%) and subsequently with the same volume of fixative containing paraformaldehyde (PAF; 4%) in phosphate buffer (PB; 0.1 M at pH 7.4). After decapitation, the brains were removed, postfixed overnight in the same fixative at 4 C, dehydrated, and embedded in Paraplast (Sherwood, St. Louis, MO). Transverse serial sections were cut at 6 μ m using a rotary microtome. One section every 60 μ m was mounted on 3-aminopropyl-triethoxylane-treated slides and then air dried at room temperature overnight. Three consecutive series covering the length of the goldfish brain were done. Two series were used for hybridization with the sense and antisense probes. The last series was stained with cresyl-violet 0.1% for detailed identification of brain nuclei. Sections were stored at 4 C under dry conditions and used for hybridization within 1 wk.

Before hybridization, sections were deparaffinized, rehydrated, and postfixed in 4% PAF for 20 min. Slides were then rinsed twice in PB for 5 min and treated with a proteinase-K solution (20 μ g/ml in 50 mM Tris-HCl, 5 mM EDTA at pH 8) for 5 min at room temperature. Slides were next washed in PB and postfixed again in PAF for 5 min, subsequently rinsed in sterile water, and acetylated in a triethanolamine (0.1 M at pH 8)/acetic anhydride solution. Sections were then dehydrated and dried at room temperature.

The entire coding region of the goldfish MC4R receptor sequence was amplified with Taq DNA (Invitrogen) using clone 931 as template. Specific H1MC4 and XhMC4 primers were used as before and low-melting-point-purified PCR fragments were subcloned into PGEM-T easy vector (Promega Corp.) and sequenced to compare against the sequence of genomic DNA clone. Both genomic and PCR-generated MC4R coding regions were identical. Antisense and sense RNA probes were then synthesized *in vitro* by linearizing the plasmid with *Nco*I and *Sall* (Invitrogen). *In vitro* transcription was carried out with SP6 or T7 RNA polymerase, respectively. Both sense and antisense probes were labeled with 10 μ l ³⁵S-uridine 5-triphosphate (³⁵S-UTP; 10 mCi/ml) using the riboprobe synthesis kit (Amersham) as described by the manufacturer. After *in vitro* RNA synthesis, samples were treated with RQ1-deoxyribonuclease (Promega Corp.) for 15 min at 37 C in presence of 50 U RNasin (Promega Corp.) and then incubated at –20 C for 3 h with 10 μ g/ml yeast RNA type III in an 8% formamide solution. Probes were subsequently purified using Sephadex G50 columns. The two fractions containing the highest radioactivity were pooled and precipitated in

FIG. 1. Nucleotide and deduced amino acid sequence of goldfish MC4R. Nucleotide and amino acid sequence numbers are indicated on the left. Underlined amino acids indicate transmembrane domains (according to Ref. 21). Open boxes frame tripeptide sequences that conform with the consensus sequence for N-linked glycosylation sites. Gray boxes enclose possible phosphorylation sites. Nucleotides in bold letters display putative polyadenylation sites, whereas nucleotides in bold italic letters conform stop codon. Sequences of primers used in RT-PCR amplification are underlined (MC4R sequence accession no. AJ534337).

-248 GAAACAGAGTTTGTGTTTTTCAGATTCA
-225 GATTTTGTGGGTGTGCGTTTTGTGTAGCCCTATCAGTTGCCGCTGTTCTGATCCTCATTCTGCATGCTTCTTTT
-150 GAGAGGCTCTTGCACCTTATCCGACCATTGGAGGTGAGGTGACAGATGCTCATAACAGCACCTGCTTTCTTTGAT
-75 CAGATGATGTTCAATTTGAATTTATCAGACTGAAGTAGATAGAGATCAAAGCACTGACTACGGATATTAGAGAA

+1 M N T S H H H G P H H **S** Y R N H S Q G A L P V G K
+1 ATGAACACCTCACATCACCATGGACCGCATCATTATACCGAAATCACAGCCAGGGGGCTTTGCCAGTGGGAAAG
MC4-DTC-F

+26 P D Q G E R G S T S G C Y E Q L L I S T E V F L T
+76 CCTGATCAAGTGAGAGAGGATCAACCTCTGGATGTTACGAGCAGCTACTCATCTCCACAGAGGTCTTCTCTACA

+51 L G L V **S** L L E N I L V I A A I I K N K N L H S P
+151 CTCGGGCTCGTCAGTCTCTGGAGAACATTTTAGTGATTGCTGCTATTATCAAGAACAAGAACCCTTCATTCTCCC

+76 M Y F F I C S L A V A D L L V S V S N A S E T V V
+226 ATGTACTTCTTTATCTGCAGTTTAGCTGTAGCAGACTGTTGGTCAGTGTCTCAAATGCCTCCGAAACGGTAGTG

+101 M A L I T G G N L I Y R E S I I K N M D N I F D S
+301 ATGGCACTCATACGGGGGGCAACCTAACTTATCGCGAGAGCATCATCAAGAACATGGACAACATTTTGGACTCG

+126 M I C S S L L A S I W S L L A I A V D R Y I T I F
+376 ATGATCTGCAGCTCACTGTTGGCCTCCATTTGGAGTTGTTGGCCATAGCGGTGGACCGCTACATCACGATCTTC

+151 Y A L R Y H N I M **T** Q R R A G T I I T C I W T L C
+451 TACGCCTTGGCGTACCACAACATCATGACCCAACGGCGGGCGGGCACCATCATCACCTGCATCTGGACCTTGTGT

+176 T V S G V L F I V Y S E S T T V L I C L I S M F F
+526 ACGGTCTCTGGCGTGCTCTTTATTTGTGTACTCTGAGAGCACCACCGTTCTCATCTGCCTTATCAGCATGTTCTTC

+201 T M L A L M A S L Y V H M F L L A R L H M K R I A
+601 ACCATGCTGGCGCTTATGGCCTCGCTCTACGTCCACATGTTTCTTCTAGCCCGGCTGCACATGAAGCGCATTGCC

+226 A L P G N G P I W Q A A N M K G A I T I T I L L G
+676 GCCCTCCCTGGCAACGGCCCTATCTGGCAGCGGCAATATGAAAGGGCCATCACTATCACTATCCTGCTGGGA

+251 V F V V C W A P F F L H L I L M I S C P R N P Y C
+751 GTATTCGTGGTGTGCTGGGCTCCCTTTTTTTTGCACCTCATCTCATGATTTCTTGCCCCGGAATCCCTATTGC

+276 I C F M S H F N M Y L I L I M C N **S** V I D P L I Y
+826 ATCTGTTTCATGTCCCACCTCAACATGTATCTGATCCTCATTATGTGCAACTCGGTATAGACCCTCTCATCTAC

+301 A F R S Q E M R K **T** F K E I C C C W Y G L A S L C
+901 GCATTACAGGACCAAGAGATGAGGAAAACCTTCAAGGAGATCTGCTGCTGCTGGTATGGACTGGCGTCTCTGTGT
MC4-DTC-R

+326 V *
+976 GTATGAAAGCTTGTCTGTTGACGTCAAAGTACTGTTGGGAGATAGATGTTGACTTGTGGATGATGCTGAGA
+1051 ATGTGGGAGATCTAATTACACTGCACAGCTTATTATTATTCTGCACACATTTATTTGATGTCCAGAGAAATGTGA
+1126 TACTATGGATGTGCTGACCATGAAAAAAAATGCTAATGTTAATGACTCAAGTATTAATTTCTTTCATTCACTG
+1201 ACATGTTCTTTTGGTGTATATATATATACACATATGATGTAACACACACACAGTCTCATTCTTTTATCTG
+1276 CTAATAAGCAAAACAAAAGTCAAAGTGCCAATATTTAAAGGCATTAATGACATAAAATGTATAGGACTGTGTG
+1351 TGTTGTGATTCACTCAAGCACAATATTTGGCTACTGTGATTATGTTCTCTCAGCAGGTGCTACTTCAGAT
+1426 ATCCAGCTCGAGAAGTATGACAGCTTAATTAATGTGTTTATACATATATATTTATTTTGTATTTTGTAAAGT
+1501 TAAGATAATTTATGTAACCTTTGTAATGCCATCTCATTGTGCAAAATAAAACAACATCAAAACAGCAAGTATGC
+1576 CTCATATATTTCTTGTGGAATTTGTAATAACAGATTTGATAGTGTGTTGATGTTTGTGCTTTTGTCTTTC
+1651 GATTTTACTTCATTTCCCTTCCCTTCCAGCTTCAAAATCATGGAGTTCAAACAGTAAATCTATATAATCTAGT
+1726 AAAAGATTGCCTGTAAGCTCTTAAAGACTATTTAGCTTTTTTTTTTTTTTTGAAGGTCATCATATTGCGCTGAAC
+1801 AGACTCTCATTGATACAACTACAAAAGGAAGGATTTCTGTGCTTGGACCTCCAATAAACTCTCATTATCCC

ethanol-sodium chloride at -20°C . The labeled probes were then stored at -20°C and used within 1 wk.

The ^{35}S -UTP riboprobes were pelleted and dissolved in an appropriate volume of 100 mM dithiothreitol (DTT) to obtain 2×10^5 cpm/ μl . After 5-min incubation at 80°C , ^{35}S -UTP riboprobes were diluted 1/10 (final concentration of probes, 10 mM DTT and 2×10^4 cpm/ μl) in hybridization buffer containing 50% formamide, 300 mM NaCl, 20 mM Tris-HCl (pH 8), 5 mM EDTA (pH 8), 10% dextran sulfate, $1 \times$ Denhardt's solution, and $0.5 \mu\text{g}/\text{ml}$ yeast RNA type III. Subsequently 100 μl hybridization solution were added to each pretreated slide (see above), which were coverslipped and incubated in a humidified chamber at 55°C overnight. The following day coverslips were removed by incubating slides into a solution containing $5 \times$ standard saline citrate buffer (SSC; $1 \times$ SSC contains 150 mM NaCl, 15 mM sodium citrate at pH 7) and 10 mM DTT for 30 min at 55°C . Slides were then rinsed in $2 \times$ SSC, 50% formamide, and 10 mM DTT for 30 min at 65°C and three times immersed into NTE buffer (500 mM NaCl; 10 mM Tris-HCl; 5 mM EDTA, pH 7.5) for 10 min at 37°C . After ribonuclease treatment ($20 \mu\text{g}/\text{ml}$ ribonuclease in NTE) for 30 min at 37°C , slides were rinsed three times in NTE buffer for 10 min at 37°C , once in $2 \times$ SSC, 50% formamide, 10 mM DTT for 30 min at 65°C , once in $2 \times$ SSC for 15 min at room temperature and twice in $0.1 \times$ SSC for 15 min at room temperature. Slides were finally dehydrated in increasing graded ethanol solutions containing 0.3 M ammonium acetate and dried at room temperature. After the hybridization process, slides were dipped in photographic emulsion (Amersham) and exposed under dry conditions at 4°C for 5–7 d, developed in D-19 (Kodak, Rochester, NY) and counterstained with toluidine blue 0.02%. Anatomical locations were confirmed by reference to a brain atlas of goldfish (28).

icv injections

Brain icv injections were performed in accordance to the methods described (28). After deep anesthesia, a three-sided flap was cut in the roof of the skull using a dentist drill equipped with a circular blade. The flap was folded to the side, thus exposing the brain. Fish were then placed in a stereotaxic apparatus, and the needle of a $5\text{-}\mu\text{l}$ Hamilton syringe was stereotaxically positioned in the hypothalamic region of the third ventricle (coordinates: $+0.2$ M, D 1.5) (28). Following the injection of $1 \mu\text{l}$ test solution, the needle was withdrawn, the cranial cavity was filled with saline 0.65%, and the skull flap was placed back in its original position and secured by surgical thread. Fish were then returned to their tanks and normally recovered from anesthesia in 1–2 min. Following this scheme, the effects on food intake were assayed over 0–2 and 0–4 h after injection of vehicle (saline 0.65%); MTII at 1- and 3-nmol dose; and HS024 at 0.8, 1.6, and 3.2 nmol doses.

Effects of MC4R agonist and antagonist on goldfish food intake

Binding and activation experiments demonstrated that MTII and HS024 act as true *in vitro* agonist and antagonist analogs of the goldfish MC4R, respectively. To corroborate *in vivo* involvement of melanocortin signaling through MC4R in the control of goldfish food intake, two experiments were carried out. The first experiment evaluated the effects of icv-injected agonist MTII on 2- and 4-h cumulative food intake of 24-h fasted animals. The second experiment studied the effects of the icv-injected antagonist HS024 on 4-h cumulative food intake of fed animals. Melanocortin analogs MTII and HS024 used in feeding experiments were purchased from Bachem (Torrance, CA), dissolved in vehicle solution (saline 0.65%) at 5 nmol/ μl , and stored at -20°C . Working aliquots for icv injections were prepared from stock solution immediately before use.

For these experiments, fish ($n = 105$, body weight = 30.48 ± 0.78 g) were individually placed into 65 liters aquaria and fed once a day (between 1030 and 1100 h) with preweighed trout pellets (between 4% and 5% body weight ration) for either 2 h or 4 h in different groups during 3 consecutive days. On the third day, food pellets that were not consumed were collected and desiccated at 100°C overnight. Food intake of unhandled animals was calculated as the difference between the initial dry weight and adjusted uneaten dry food weight. The reduction in weight of food remaining in water for either 2 h or 4 h and desiccated in parallel with the experimental samples was used to adjust the uneaten

dry food weight from the experimental aquaria (29). On the fourth experimental day, fish were carefully removed from the tanks, anesthetized, icv injected with test solution, and subsequently returned to their home tanks. Fish were then allowed to recover during 15 min, and subsequently preweighed food pellets (5–6% body weight ration) were added to the tank. Unfed pellets were collected after 2 or 4 h and food intake was calculated as before. Following this protocol the effect of vehicle after 2 ($n = 18$) and 4 h ($n = 8$) post injection and MTII at 1 (2 h, $n = 11$; 4 h, $n = 10$) and 3 nmol (2 h, $n = 11$; 4 h, $n = 10$) were evaluated.

For the second experiment, fish were treated as before and allowed to eat for 4 h during 3 consecutive days. On the fourth experimental day, fish were allowed to feed for 3 h, and then they were icv injected. Following icv injections fish were returned to their respective aquaria. Food pellets not consumed were collected after 4 h, and food intake was calculated as before. Following this schedule the effect of vehicle ($n = 13$) and HS024 icv injection at 0.8 ($n = 9$), 1.6 ($n = 8$), and 3.2 nmol ($n = 7$) were tested.

Tests were carried out in random order in terms of treatment and days. Food intake levels and body weight are expressed as mean \pm SE of the mean (SEM). Differences between control and experimental groups were determined by ANOVA followed by Duncan's multiple range tests. Differences in food intake between the unhandled previous day and experimental day were tested by paired-samples *t* test. Statistical significance was considered at $P < 0.05$.

Results

Molecular cloning of goldfish MC4R

By screening a goldfish genomic library with a zebrafish MC4R probe, we isolated and purified seven positive clones containing fragments of about 12–15 kb. After restriction and Southern blot analysis, clones 931 and 1648 were selected for further characterization and sequencing. Both the 931 and 1648 clones were found to contain identical open reading frames of 981 bp encoding a putative 326-amino acid protein with seven potential hydrophobic transmembrane domains (TMDs), a particular characteristic of G protein-coupled receptors (Fig. 1). As with many G protein-coupled receptors, the coding region of the putative goldfish receptor was intronless. Typical sequences characteristic of the promoter region, such as TATA-box and CCAAT-box, could not be recognized within 248 bp upstream from the putative translation initiation site. In the 3' downstream from the coding region, there are two potential poly (A) signals at positions 1812–1817 and 2123–2128 (Fig. 1).

The deduced amino acid sequence is 68% and 96% identical with human and zebrafish MC4R, respectively (Fig. 2). However, it is 61% identical with human MC5R and 65% and 64% identical with both zebrafish MC5R (zMC5R) versions, *i.e.* zMC5Ra and zMC5Rb, respectively (Fig. 2). The identity is unevenly distributed, and the N-terminal extracellular domain displays the lowest identity level to other MC4Rs, including zebrafish MC4R. More than 50% divergence between zebrafish and goldfish MC4R orthologs resides within the N-terminal domain, encoding only 14% of total protein length. A more detailed comparison shows that the overall identity level of goldfish receptor to other MC4Rs within TMD5, TMD6, and TMD7 is higher than 92% and higher than 73% within TMD1 and TMD4, respectively.

Similar to other MCRs, goldfish MC4R ortholog exhibits short extracellular (ECL) and intracellular (ICL) loops and substitution of a methionine for proline in the fifth transmembrane domain (TM5) and shares cysteine residues at positions 255, 269, and 275, which are fully conserved in all MCRs (Fig. 2 and <http://www.gpcr.org>). In addition, gold-

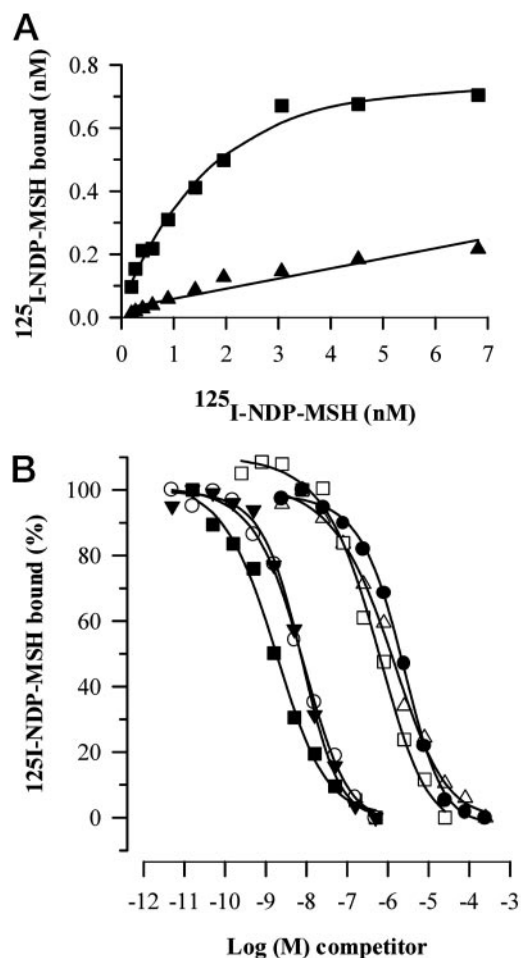


FIG. 3. Saturation and competition curves for goldfish MC4R expressed in intact transfected cells. A, Saturation curve were obtained with NDP-MSH and the figure shows total binding (■) and binding in the presence of 2 μ M cold NDP-MSH (▲). Lines represent the computer-modeled best fit of the data assuming that ligands bound to one site. B, Competition curves for NDP-MSH (■), α -MSH (Δ), β -MSH (\square), γ -MSH (\bullet), MTII (\circ), and HS024 (\blacktriangledown) were obtained by using a fixed concentration of 2 nM NDP-MSH and varying concentrations of the nonlabeled competing peptide. Each point represents average \pm SEM (n = 6).

TABLE 1. K_i and K_d values (mean \pm SEM) from respective competitive and saturation curves for melanocortin analogs on goldfish MC4R-transfected HEK-293 EBNA cells

Ligand	g-MC4R (nM)	z-MC4R (nM)	h-MC4R (nM)
[125 I]NDP-MSH (K_d)	1.25 \pm 0.08	2.39 \pm 0.96 ^a	2.35 \pm 1.18 ^a
NDP-MSH (K_i)	1.43 \pm 0.04	3.35 \pm 0.31 ^a	3.57 \pm 0.30 ^a
α -MSH (K_i)	988 \pm 74	243 \pm 27 ^a	289 \pm 29 ^a
β -MSH (K_i)	391 \pm 39	163 \pm 14 ^a	126 \pm 15 ^a
γ 1-MSH (K_i)	2310 \pm 293	2200 \pm 550	3690 \pm 260 ^a
HS024 (K_i)	4.57 \pm 0.42	ND	0.29 \pm 0.14 ^b
MTII (K_i)	5.62 \pm 0.52	ND	6.60 \pm 0.82 ^c

^a Results taken from Ref. 21; ^b results taken from Ref. 59; ^c results taken from Ref. 18. ND, Not determined; g-, goldfish; z-, zebrafish; h-, human. K_i , Inhibition constant; K_d , dissociation constant.

cells were incubated with increasing concentrations of MTII and a fixed concentration of HS024, the MTII-EC₅₀ was shifted to 138 \pm 5.9 nM. The latter result indicates that HS024 inhibits MTII-stimulated cAMP ICL accumulation in

HEK239-EBNA cells transfected with goldfish MC4R as would have been expected for a functional antagonist.

Peripheral and central distribution of MC4R mRNA

RT-PCR with specific primers respectively targeting ECL (MC4-DTC-F primer) and ICL (MC4-DTC-R) tails of the goldfish MC4R (Fig. 1) resulted in a band of the expected size of about 0.95 kb (Figs. 5A and 6A). The identity of the band was confirmed by Southern blot hybridization with a goldfish MC4R probe including the full coding region (Figs. 5B and 6B). Goldfish MC4R mRNA was detected in the retina, dorsal skin, gill, spleen, ovary, and all brain regions, with residual levels in the olfactory bulb (Figs. 5, A and B, and 6, A and B). No bands or hybridization signal for goldfish MC4R were obtained in PCR using ventral skin, heart, kid-

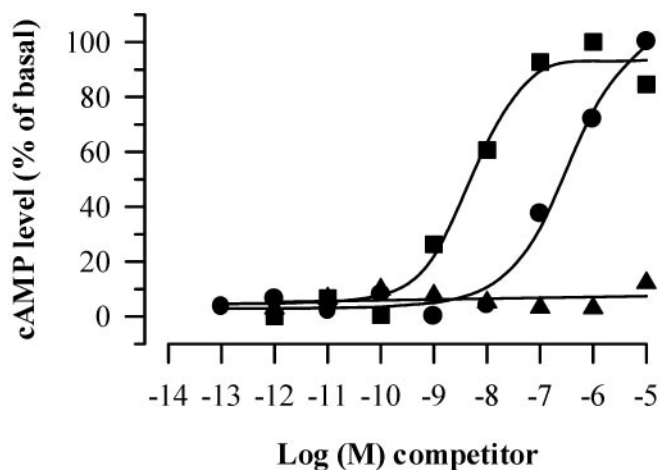


FIG. 4. Generation of cAMP in response to MTII (■), HS024 (▲), and MTII plus constant concentration of 0.1 μ M HS024 (●) for goldfish MC4R receptor in transfected HEK293-EBNA cells. Untransfected HEK293-EBNA cells showed no cAMP response to MTII (data not shown). Each point represents average \pm SEM (n = 6).

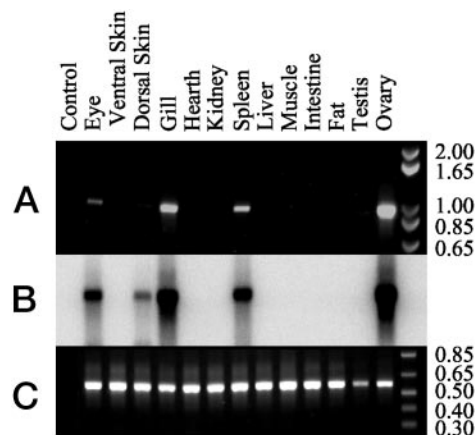


FIG. 5. Distribution of goldfish MCR4 mRNA expression in different tissues as revealed by RT-PCR assay followed by Southern blot hybridization. A, Ethidium bromide-stained agarose gels of RT-PCR amplifications carried out with primers set MC4-DTC-F and MC4-DTC-R. B, PhosphorImaging screen of Southern blot analysis with a probe including full coding region of the goldfish receptor following RT-PCR assays. C, Ethidium bromide-stained agarose gels of RT-PCR amplifications carried out with primers set actin 1 and actin 2 (26).

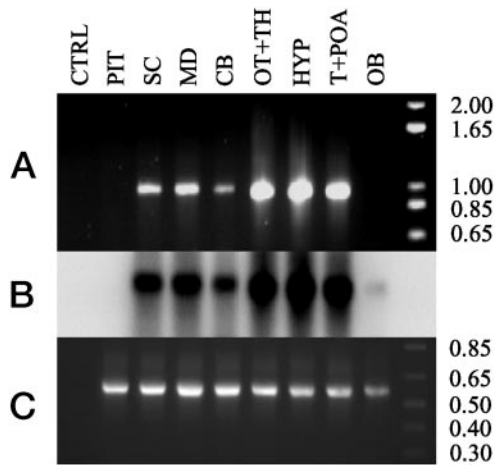


FIG. 6. Distribution of goldfish MCR4-mRNA expression in discrete brain section as revealed by RT-PCR assay followed by Southern blot hybridization. A, Ethidium bromide-stained agarose gels of RT-PCR amplifications carried out with primers set MC4-DTC-F and MC4-DTC-R (Fig. 1). B, PhosphorImaging screen of Southern blot analysis with a probe including full coding region of the goldfish receptor following RT-PCR assays. C, Ethidium bromide-stained agarose gels of RT-PCR amplifications carried out with primers set actin 1 and actin 2 (26). OB, Olfactory bulbs; T+POA, telencephalon + preoptic area; HYP, hypothalamus; OT+TH, optic tectum + thalamus; CB, cerebellum; MD, medulla; SC, spinal cord; PIT, pituitary; CTRL, negative control, no cDNA.

ney, liver, muscle, intestine, fat, testis, and pituitary cDNA or water (control) as template (Fig. 5, A and B). Inverse transcriptions and cDNA quality were corroborated by PCR amplification of β -actin cDNA that yielded bands of expected size in all reactions (Figs. 5C and 6C).

To further characterize neuronal expression of MC4R mRNA, we used the *in situ* hybridization technique. Hybridization with sense MC4R-cRNA probes never generated specific signals in the goldfish brain (data not shown), supporting the probe specificity. Figure 7 schematically represents the distribution of MC4R mRNA within goldfish brain. Cells groups expressing MC4R mRNA were detected in the following areas: telencephalon, preoptic area, hypothalamus, and ventral thalamus. The first MC4R-expressing neurons were localized within the rostral-most area of the medial part of the dorsal telencephalon (Dm, Figs. 7A and 8A). At this same brain level, some perikarya could also be observed in the ventral area of the central part of the dorsal telencephalon (Dc, Fig. 7A) as well as within the lateral lining of the lateral part of the dorsal telencephalon (Dl, Fig. 7A). More caudally a conspicuous MC4R mRNA-expressing neuronal population was located within the ventral part of the ventral telencephalon (Vv, Figs. 7B and 8B). At this level, some perikarya can be also observed within the central part of the dorsal telencephalon and the lateral lining of the lateral part of the dorsal telencephalon (Fig. 7B).

Positive MC4R-labeled neurons were evident in several parts of the preoptic area. MC4R mRNA-expressing cells appear in the periventricular part of the preoptic nucleus (NPP, Figs. 7C and 8C). In the latter nucleus, the profuse MC4R expression adopts a periventricular disposition, and almost all neurons seem to be melanocortin dependent. Slightly more caudal, a profuse MC4R mRNA expression

was found in the magnocellular neurons of the preoptic nucleus (NPO, Figs. 7D and 8D). Neurons expressing MC4R mRNA within the latter division appear to be restricted to the lateral area of the nucleus far from the medial periventricular area (Fig. 8D). Caudally MC4R expression can also be detected within the anterior periventricular nucleus (NAPv) and in the ventrolateral pole of the preoptic recess coinciding with the suprachiasmatic nucleus (SCN, Figs. 7E and 8E). At this level MC4R mRNA-expressing neurons of the preoptic nucleus (NPO) adopt a more periventricular location (Fig. 8E).

Within the tuberal hypothalamus, almost all divisions were found to profusely produce MC4R mRNA. MC4R mRNA-expressing neurons were found in the tuberal hypothalamus in the anterior part of the lateral tuberal nucleus (NLTa, Fig. 7D). At this level, some positive perikarya could be observed in the medial area of the anterior hypothalamic nucleus (NAH, Fig. 7D), also named the anterior pregglomerular nucleus in other species (30). MC4R-expressing neurons of the NLTa are continuous with those within the posterior part of the lateral tuberal nucleus (NLTp) and the anterior tuberal nucleus (NAT, Figs. 7E and 8F). In the NLTp, MC4R neurons line the third ventricle and most periventricular neurons appear to make contact with the cerebrospinal fluid (data not shown). More caudally, MC4R neurons are located in the lateral recess nucleus lining the lateral hypothalamic recess (Fig. 7F). Some large MC4R positive perikarya were also detected within the diffuse nucleus of the inferior lobe of the hypothalamus (NDLI, Fig. 7G) coinciding with the central nucleus of the inferior lobe of other species (30). Finally, in the thalamus, MC4R mRNA-expressing neurons were restricted to the ventromedial nucleus of the ventral thalamus (Fig. 7, F and G).

Effects of agonist and antagonist analogs of goldfish MC4R on food intake

No differences in food intake were detected between groups of unhandled animals (Fig. 9, A and B). Saline injection had no effect on 2- and 4-h cumulative food intake in 24-h fasted animals (Fig. 9, A and B). The icv injections of the goldfish MC4R agonist MTII at doses of 1 and 3 nmol caused a dose-dependent decrease in 2-h cumulative food intake (Fig. 9A). Only the high dose of 3 nmol caused a significant decrease in 4-h cumulative food intake (Fig. 9B). The icv injection of the goldfish MC4R antagonist, HS024, significantly increased 4-h cumulative food intake in previously fed animals (Fig. 10).

Discussion

The present study strongly supports the participation of the MC4R in the control of energy balance in the goldfish. Our results demonstrate that MC4R is profusely expressed within neuroendocrine- and food intake-controlling pathways of the goldfish brain. Pharmacological studies characterized functional agonist and antagonist analogs of MC4R that inhibited or stimulated food intake, respectively, when centrally administered to 24-h fasted and fed fish. The results suggest that the central melanocortin system may have

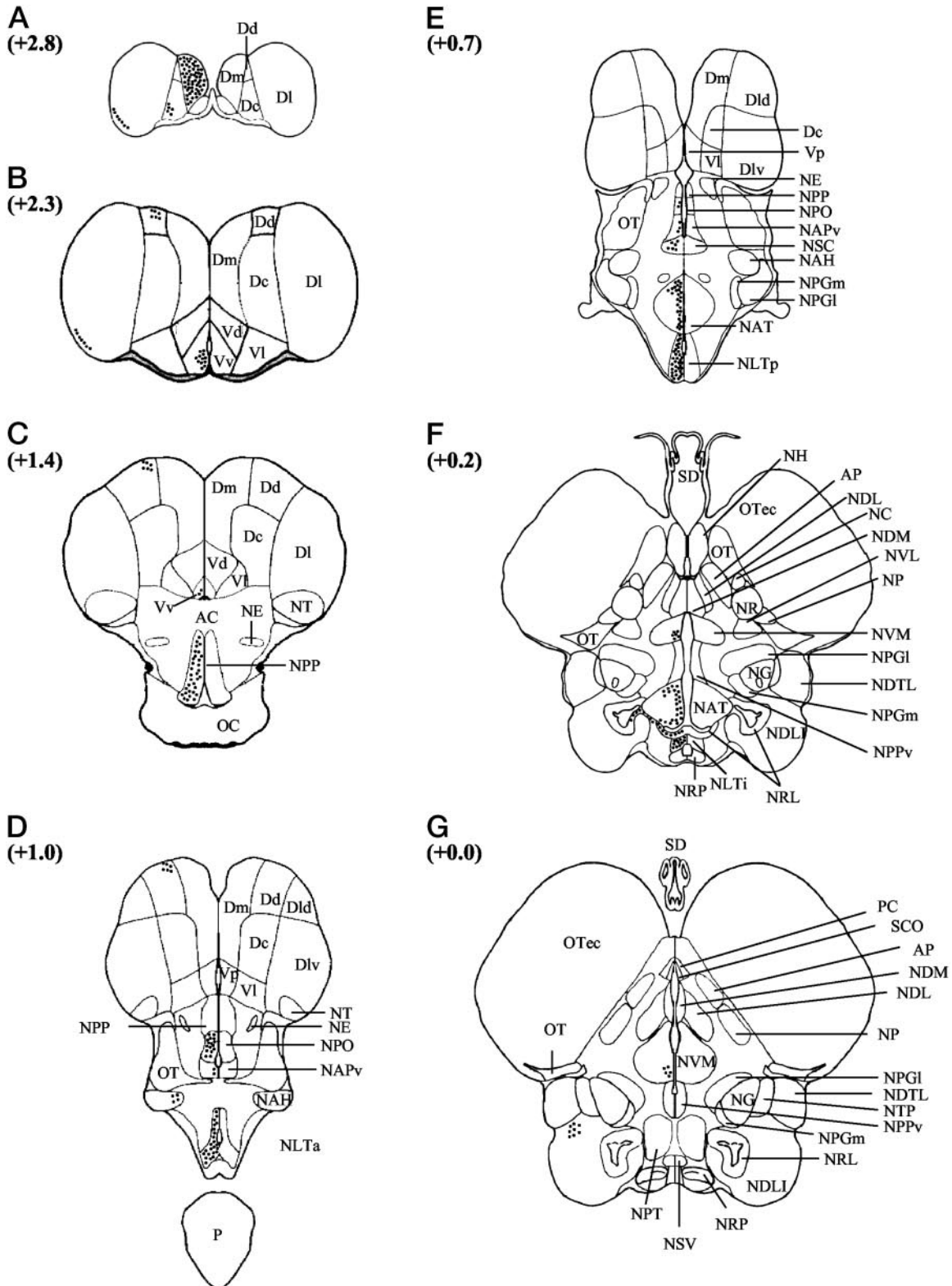


FIG. 7. A–G, Schematic drawings of the successive rostrocaudal transverse sections of the goldfish brain showing the distribution of MC4R-expressing perikarya (black dots) as revealed by *in situ* hybridization. Number of dots roughly represents expression density, but quantitative studies were not done. Numbers indicate relative location (mm) to the anterior-posterior zero point of the stereotaxic atlas set at the anterior

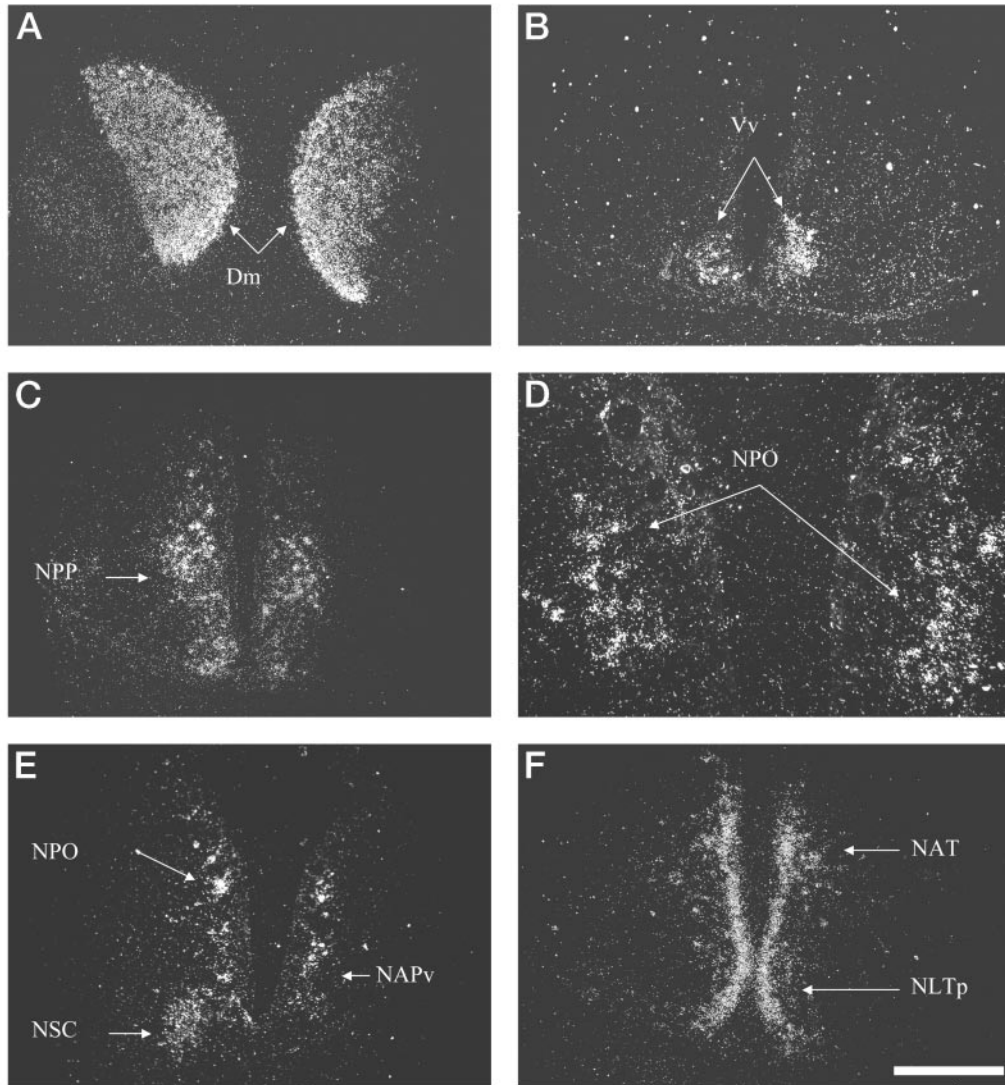


FIG. 8. Dark-field photomicrographs of transverse sections of the goldfish brain from rostral telencephalon (A) to mediobasal hypothalamus (F). A, Positive MCR4 neurons placed within the rostra-most aspect of the rostral area of the medial part of the dorsal telencephalon (Dm). B, MC4R-expressing neurons at the ventral part of the ventral telencephalon (Vv). C, MC4R neurons at the rostral division of the preoptic area within NPP. D, MC4R expression at the magnocellular bodies of the NPO. E, Photomicrography slightly caudal to D showing MC4R expression within NPO, NAPv, and suprachiasmatic nucleus (NSC). F, Profuse MC4R expression within lateral tuberal nucleus of the mediobasal hypothalamus (NLT). Scale bar, 200 μ m except 100 μ m for D.

a tonic inhibitory input on food intake, which can be overcome by central administration of MC4R antagonists.

Sequence comparisons revealed that the cloned receptor in

goldfish shares a much higher identity level to zebrafish MC4R (96%) than to zebrafish MC5Ra (65%) or MC5Rb (64%). Both zebrafish MC4R and MC5R have previously also

midmargin of the posterior commissure (28). Scale bar, 1 mm. AC, Anterior commissure; AP, prepectal area; Dc, central part of the dorsal telencephalon; Dd, dorsal part of the dorsal telencephalon; Dl, lateral part of the dorsal telencephalon; Dld, laterodorsal part of the dorsal telencephalon; Dlv, lateroventral part of the dorsal telencephalon; Dm, medial part of the dorsal telencephalon; NAH, anterior hypothalamic nucleus; NAT, anterior tuberal nucleus; NC, cortical nucleus; NDL, dorsolateral nucleus of the dorsal thalamus; NDLI, diffuse nucleus of the inferior lobe; NDM, dorsomedial nucleus of the dorsal thalamus; NDTL, diffuse nucleus of the lateral torus; NE, entopeduncular nucleus; NG, glomerular nucleus; NH, habenular nucleus; NLTa, anterior part of the lateral tuberal nucleus; NLTi, inferior part of the lateral tuberal nucleus; NP, prepectal nucleus; NPGl, lateral part of the preglomerular nucleus; NPGm, medial part of the preglomerular nucleus; NPPv, posterior periventricular nucleus; NPT, posterior tuberal nucleus; NR, nucleus rotundus; NRL, lateral recess nucleus; NRP, posterior recess nucleus; NSC, suprachiasmatic nucleus; NSV, nucleus of the vascular saccus; NT, nucleus taenia; NVL, ventrolateral nucleus of the ventral thalamus; NVM, ventromedial nucleus of the ventral thalamus; OC, optic chiasma; OT, optic tract; OTec, optic tectum; P, pituitary; PC, posterior commissure; SCO, subcommissural organ; SD, saccus dorsalis; Vd, dorsal part of the ventral telencephalon; Vl, lateral part of the ventral telencephalon; Vp, postcommissural part of the ventral telencephalon; Vs, supracommissural part of the ventral telencephalon; Vv, ventral part of the ventral telencephalon.

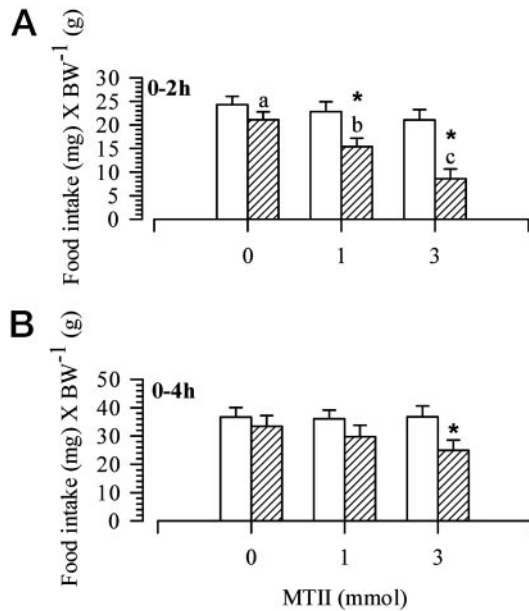


FIG. 9. Effects of icv injection of melanocortin agonist MTII on cumulative food intake of 24-h fasted goldfish. On d 1, food intake of unhandled animals was recorded during a 2-h (A) or 4-h (B) period. On d 2, same fishes were injected with saline ($n = 8$ at 2 h and $n = 8$ at 4 h) MTII at 1 ($n = 11$ at 2 h and $n = 10$ at 4 h) and 3 nmol ($n = 11$ at 2 h and $n = 10$ at 4 h). Fish received food 15 min after icv and then were allowed to eat during the following 2 or 4 h. At the end of the 2- or 4-h period, remaining pellets were recovered, desiccated at 100 C, and weighed. Data (mean \pm SEM) represent cumulative food intake at 0–2 and 0–4 h after presentation of food. Dissimilar superscripts indicate significant differences (one-way ANOVA, $P < 0.05$) from the saline-treated group. Asterisks indicate significant differences ($P < 0.05$) after paired *t* test of treated animals, compared with food intake values of unhandled animals at d 1.

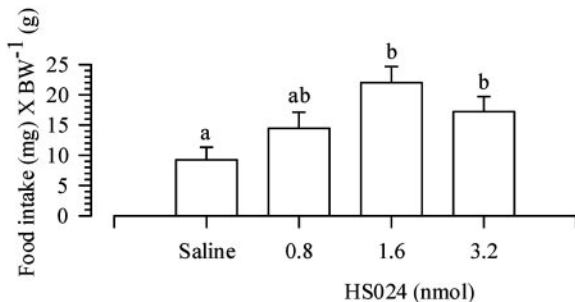


FIG. 10. Effects of icv injection of melanocortin MCR4 antagonist HS024 on accumulative food intake of fed goldfish. On the experimental day, fish ate for 3 h and then were icv injected with saline ($n = 13$) or HS024 at 0.8 ($n = 9$), 1.6 ($n = 8$), and 3.2 nmol ($n = 7$). Fifteen minutes after surgery fish received food and then were allowed to eat during 4 h. Data (mean \pm SEM) represent cumulative food intake at 0–4 h after presentation of food. Dissimilar superscript letters indicate significant differences (one-way ANOVA, $P < 0.05$) from the saline-treated group.

been shown to display strong phylogenetic relationships to their respective mammalian counterparts (21). Phylogenetic analysis supports evidence that this new gene is a MC4R ortholog (data not shown). Most of the divergence in goldfish MC4R is within the N-terminal ECL domain. However, the latter receptor domain is not likely to be structurally and functionally important for MC4R activity because it has been

demonstrated that 28 amino acids from N-terminal ECL domain can be deleted, including all potential N-glycosylation sites, without affecting ligand binding to human MC4R (31). In contrast, goldfish MC4R shares a high identity level to other MC4Rs within the TMDs. Point mutagenesis and molecular modeling of human MC1R suggests that important determinants for agonist binding (NDP-MSH and MTII) lie within the TMDs (5, 32). Three-dimensional modeling suggests that a series of amino acid residues in TMD2 (E94), TMD3 (D117, D121), and TMD7 (F280, N281) (E97, D120, D124, F282, N283, goldfish MC4R numbering) form a hydrophilic-binding pocket for interaction with positively charged amino acids of NDP-MSH sequence. Similarly, the aromatic series in the TMD4 (F175, F179, Y182, Y183), TMD5 (F195 and F196), and TMD6 (F257 and F258) (S178, F182, Y185, S186, M198, F199, F259, F260 goldfish MC4R numbering) provide a hydrophobic binding pocket for aromatic-aromatic interactions with amino acid residues in NDP-MSH (5, 32). Except for F175, Y183, and F195 that respectively correspond to S178, S186, and M198 of the goldfish MC4R, all above residues thought to form hydrophilic and hydrophobic pockets are conserved in the goldfish MC4R.

Binding experiments show that goldfish MC4R binds both melanocortin mimetics, NDP-MSH and MTII, within the nanomolar range. Although the mammalian MCR subtypes, except for MC2R, are promiscuous in activation by melanocortins, each one has its own profile of activation (5, 6). Goldfish MC4R shares the distinctive characteristics of human and zebrafish MC4R, *i.e.* low affinity for γ -MSH and a higher or similar affinity for β -MSH, compared with α -MSH. Interestingly, the γ -MSH domain in POMC occurs only as a remnant in primitive actinopterygians, but it is absent in the teleost fish, including goldfish (33). The physiological role of β -MSH is still unclear despite its high degree of evolutionary conservation, which presumes a conserved function. Higher affinity of β -MSH than α -MSH to both zebrafish and goldfish MC4R further suggests that a specific role of β -MSH for this receptor subtype could be evolutionary conserved. Similar to all reported MCRs, goldfish MC4R is positively coupled to the cAMP-signaling pathway, in response to the nonselective melanocortin agonist MTII. Moreover, MTII-stimulated cAMP ICL accumulation decreases by coincubation with HS024. The latter compound binds to goldfish MC4R with comparable affinity to MTII, thus demonstrating that it is a functional and suitable antagonist. Interestingly, goldfish MC4R displays similar affinity to MTII, compared with the human counterpart, but the latter receptor exhibits about a 10-fold higher affinity for HS024 than the goldfish MC4R. This suggests that the three-dimensional binding pocket in goldfish MC4R is well fitted to bind MTII. Nevertheless, our data show that HS024 is suitable for physiological studies in goldfish, as previously shown in rat (18).

In mammals, MC4R is expressed within the CNS and it is essentially absent in the periphery. However, in chicken MC4R-mRNA, production in ovary, testis, spleen, adipose tissue (34), and eye (35) has been reported. Furthermore, peripheral expression of MC4R mRNA was also detected in the ovary, gastrointestinal tract, and eye of the zebrafish (21). Our study demonstrates MC4R expression, by RT-PCR, in the goldfish ovary, spleen, gill, retina, and all brain regions,

supporting that neural specificity of MC4R is a derived character in mammalian lineage. Of special interest was the distribution of MC4R in the skin. RT-PCR experiments in the goldfish demonstrated expression of MC4R in the dorsal skin, but no expression was found in the ventral skin. Similar to many other vertebrates, common goldfish have a specific pigment pattern revealing red color in the dorsal area and a progressive gradation toward white-yellow tones in the abdominal skin. Differential MC4R expression in the dorsal skin further supports a role in pigment synthesis and suggests that MC4R may be involved in the color patterning of the goldfish.

To further understand the role of central MC4R signaling in nonmammalian vertebrates, we studied MC4R-mRNA distribution in goldfish brain by *in situ* hybridization. Receptor transcripts were restricted to the forebrain, including dorsal and ventral telencephalon, preoptic area, ventral thalamus, tuberal hypothalamus, and hypothalamic inferior lobe. By RT-PCR, low levels of MC4R transcript were additionally detected within cerebellum, medulla, and spinal cord. Goldfish MC4R-mRNA distribution within the CNS fits well with previous immunocytochemical studies on the distribution of ACTH-like immunoreactive fibers in the goldfish brain (36). Briefly, the density of the ACTH-like fiber network was maximal in the ventral hypothalamus, particularly in the median part of the lateral tuberal nucleus, in which a high level of MC4R expression was also found. The ACTH-like fiber network extended around the lateral and posterior hypothalamic recess and toward the dorsal thalamus. In agreement with this, MC4R-mRNA expression was found in the lateral recess nucleus and central nucleus of the inferior lobe. We found MC4R to be profusely expressed within almost all divisions of the preoptic area, including the NPP, the parvo- and magnocellular neurons of the preoptic nucleus, NAPv, and in the ventrolateral pole of the preoptic recess, coinciding with the suprachiasmatic nucleus. In the telencephalon, immunoreactive fibers are located ventromedially, showing a dense network in the prechiasmatic area, and some fibers are also detected in the mediodorsal telencephalon. Correspondingly, profuse MC4R expression was found in the medial part of the dorsal telencephalon, and a concise MC4R-expressing neuronal group was found in the ventral part of the ventral telencephalon, which is prechiasmatically positioned. Comparative studies are difficult because detailed distribution of MC4R expression has been described only in the rat brain (4, 37, 38). In this species, MC4R transcripts are localized within more than 100 different discrete structures that extend through each major division of the brain. MC4R-mRNA is profusely expressed in the rat hypothalamus including anteroventral periventricular, ventromedial preoptic, median preoptic, paraventricular, dorsomedial, and arcuate nuclei. The subfornical organ, dorsal hypothalamic, perifornical and posterior hypothalamic areas are also observed to express MC4R-mRNA. High expression levels are detected in extrahypothalamic areas including tubercle olfactory, caudoputamen, lateral septal nucleus, amygdala, and lower levels are found in the thalamus and bed nucleus of the stria terminalis.

Homology relationships between fish and mammalian nuclei are complex. The hypothalamic region appears to be

highly variable among the different anamniotic radiations, and it is presently difficult to homologize many of the nuclei across gnathostomes (39). However, the lateral tuberal nucleus is thought to be the teleostean homolog of the mammalian arcuate nucleus and the parvo- and magnocellular neurons of the preoptic nucleus are homolog of the mammalian supraoptic and paraventricular nuclei. The ventral area of the ventral telencephalon (Vv), in which MC4R is profusely expressed in the goldfish brain, is a homolog to the mammalian lateral septal nucleus (39). Within the septum of the rat brain, the lateral septal nucleus displays the densest MC4R hybridization level. The dorsoposterior zone of the dorsal telencephalon in the goldfish is homologous to the primary olfactory cortex in which moderate MC4R expression was found in the rat brain. The dorsomedial area of the dorsal telencephalon (Dm) has been suggested to be a limbic-like zone of the teleostean telencephalon, and it could be homologous to the mammalian pallial amygdala (40). Overall, this suggests that hypothalamic MC4R expression has been well conserved throughout the vertebrate evolutionary process. However, the more extensive expression of MC4R mRNA in the rat brain suggests the acquisition of new central functions for MC4R in the mammalian lineage.

MC4R is localized in areas appropriate for control of the hypothalamic-pituitary axis because the preoptic area and tuberal hypothalamus are the main hypophysiotropic areas of the goldfish brain (41). It has been demonstrated that magnocellular neurons of the NPO profusely produce NPY (42), and NPY stimulates both LH and GH secretion either directly on the gonadotropic cells or through presynaptic stimulation of GnRH release (43). This suggests that melanocortin may modulate NPY expression and/or release from the preoptic area, therefore controlling reproductive and growth processes in the goldfish. In addition, GHRH immunoreactivity has been demonstrated within the NPP and lateral tuberal nucleus (NLT) (44), areas in which we describe profuse expression of MC4R. Both NPP and NPO are also the main corticotrophin-releasing hormone-producing areas in the brain of cyprinid fish, including goldfish (45). This neuropeptide is involved in the stress activation of hypothalamic-pituitary-interrenal axis, which severely affects fish growth (46). Although the involvement of the central melanocortin system in goldfish is unknown, it is known that MC4R knockout mice, agouti yellow mice, and AGRP transgenic mice, each of which is melanocortin signaling deficient, exhibit enhanced growth (10, 11, 13).

Central neuronal pathways involving energy homeostasis in fish are not well defined. It is generally accepted that hypothalamic inferior lobe, particularly areas placed closely to the hypothalamic lateral recess, as well as the ventroposterior hypothalamus, are involved in the control of food intake. The latter areas form a hypothalamic center in which food intake is modified according to visceral and sensorial incoming information (47). It has been demonstrated that electrical stimulation in the region surrounding the hypothalamic lateral recess induces a feeding response in bluegill (*Lepomis macrochirus*; Ref. 48). However, the latter area is part of a widespread neuronal system because electrical stimulation of the ventral telencephalon and glomerular nucleus (currently tertiary gustatory nucleus) evokes feeding and

aggressive responses in the latter species (48). The inferior lobe is integrated within the topology of the gustatory, visual, and auditory systems of the goldfish brain, and it is thus thought to be a multisensory integration center (49). Therefore, the inferior lobe likely plays an important role integrating sensory information and possibly releasing an orchestrated feeding response. The preoptic area also forms part of the neural system involved in energy homeostasis because *in situ* hybridization studies reported increased NPY-like expression within the preoptic nucleus in fasted salmon (50, 51). Central administration of NPY has been shown to stimulate food intake in the goldfish (52). Our results confirm that MC4R is expressed within main brain areas affecting food intake in fish because transcripts were detected within ventral telencephalon, preoptic area, inferior lobe, and lateral tuberal nucleus.

The doses of melanocortin mimetics that were effective in modulating food intake in this study were in the low nanomolar range. A dose-dependent inhibitory effect of MTII was observed during the first 2 h following treatment. However, only the higher MTII doses induced a significant decrease in food intake 4 h after treatment, compared with the levels exhibited by the same unhandled animals the day before. Central administration of HS024 to fed animals stimulated increased food intake up to 4 h after treatment. Similar results have been reported in rodents icv injected with MTII (17) or HS024 (18). The melanocortin mimetic MTII is a full agonist at all characterized MCRs in rodents and humans (17). It is therefore not possible to infer the subtype of receptor involved in melanocortin actions by using the latter agonist. However, HS024 is a highly specific antagonist at rat (53) and human MC4R (18), and goldfish MC4R shares a similar binding and activation pattern as the mammalian MC4Rs. MTII activates goldfish MC4R as demonstrated by increased levels of ICL cAMP, whereas HS024 inhibits MTII-stimulated cAMP accumulation. The results therefore strongly suggest a role for central MC4R in the control of food intake in the goldfish. However, because central MCRs have not been fully characterized in the goldfish, we cannot rule out the participation of additional MCRs in the control of food intake. We have previously described MC5R expression within zebrafish brain (21). Preliminary studies in goldfish have also characterized central expression of MC5R, and pharmacological studies demonstrated that HS024 is an agonist at the latter receptor (Cerdá-Reverter, J. M., M. Ling, H. B. Schiöth, and R. E. Peter, unpublished results). In mammals, MC3R has been shown to be involved in the regulation of energy balance (12). However, melanocortin effects on food intake seem to be due exclusively to MC4R because MC4R knockout mice are insensitive to anorexic effects of centrally administered MTII (19).

Involvement of the melanocortin system in the control of energy balance of fish is corroborated by the cobalt phenotype of rainbow trout, so named because of their cobalt-blue body color. This phenomenon has been attributed to the absence of most of the pars intermedia of the pituitary, in which α -MSH is synthesized. This variant of trout is hyperphagic and typically also has an enlarged liver and fat accumulation in the abdominal cavity, reflecting the absence of α -MSH lipolytic activity (54). This suggests that the melano-

nocortin system plays a dual role in the control of energy balance by activating peripheral lipolytic activity and thus enhancing energy expenditure and by central inhibition of food intake. Previous studies in the goldfish brain have revealed that POMC is exclusively expressed within the lateral tuberal nucleus (homolog to mammalian arcuate nucleus), but progressive fasting up to 7 d does not significantly modify hypothalamic mRNA levels (Cerdá-Reverter, J. M., H. B. Schiöth, and R. E. Peter, unpublished results). Antagonist data and POMC expression levels in goldfish together with the obese phenotype exhibited by cobalt trout argues that endogenous POMC neurons may exert a tonic inhibitory effect on feeding and energy storage via release of α -MSH at sites expressing MCRs.

In conclusion, we show that there exists an evolutionarily highly conserved MC4R gene in goldfish. The receptor shows pharmacological characteristics similar to its human ortholog for the natural α -, β -, and γ -MSH analogs. Moreover, we identified MTII and HS024 as highly potent agonist and antagonist analogs, respectively, suitable to clarify the physiological functions of this receptor. We have also shown that the MC4R is abundantly expressed within goldfish brain, and expression was also found in some peripheral tissues such as ovary, spleen, and gill, indicating that the receptor may have additional functions in lower vertebrates, compared with mammals. We have performed the first detailed brain mapping of the MC4R in a nonamniote species. The results show that MC4R-mRNA is localized in key areas for neuroendocrine and food intake control of the goldfish brain. Our behavioral testing suggests that melanocortins exert an inhibitory action on food intake, which seems to be mediated at least in part by central MC4R signaling. The conserved central expression patterns of MC4R-mRNA and the effects of MC4R analogs on physiological regulation of food intake suggest that the neuronal pathways of melanocortin evolved early in vertebrate evolution and are thus likely to be important for regulation of energy homeostasis across vertebrate phylogeny.

Acknowledgments

Received December 30, 2002. Accepted February 10, 2003.

Address all correspondence and requests for reprints to: Dr. J. M. Cerdá-Reverter, Department of Fish Reproductive Physiology, Instituto de Acuicultura de Torre de la Sal, 12595 Torre de la Sal, Ribera de Cabanes, Castellón, Spain. E-mail: cerdarev@iats.csic.es.

This work was supported by Natural Science and Engineering Research Council of Canada Grant A6371 (to R.E.P.), Killam Trust Association (to J.M.C.-R.), Swedish Research Council (VR, Medicine), and Melacure Therapeutics AB (to H.S.).

J.M.C.-R. was recipient of a Killam Postdoctoral Fellowship from Killam Trust Association.

References

1. Kalra SP, Dube MG, Pu S, Xu B, Horvath TL, Kalra PS 1999 Interacting appetite-regulating pathways in the hypothalamic regulation of body weight. *Endocr Rev* 20:68–100
2. Marks DL, Cone RD 2001 Central melanocortins and the regulation of weight during acute and chronic disease. *Recent Prog Horm Res* 56:359–375
3. Castro MG, Morrison E 1997 Post-translational processing of proopiomelanocortin in the pituitary and the brain. *Crit Rev Neurobiol* 11:35–57
4. Bangol D, Lu X-Y, Kaelin CB, Day HEW, Ollmann M, Gantz I, Akil H, Barsh GS, Watson SJ 1999 Anatomy of an endogenous antagonist: relationship

- between agouti-related protein and proopiomelanocortin in the brain. *J Neurosci* 19:RC26
5. Cone RD, Lu D, Koppula S, Vage DI, Klungland H, Boston B, Chen W, Orth DN, Pouton C, Kesterson RA 1996 The melanocortin receptors: agonists, antagonists, and the hormonal control of pigmentation. *Recent Prog Horm Res* 51:287–317
 6. Schiöth HB 2002 The physiological role of melanocortin receptors. *Vitam Horm* 63:195–232
 7. Cone RD 1999 The central melanocortin system and energy homeostasis. *Trends Endocrinol Metab* 10:211–216
 8. Wilson BD, Ollmann MM, Barsh GS 1999 The role of agouti-related protein in regulating body weight. *Mol Med* 5:250–256
 9. Dinulescu DM, Cone RD 2000 Agouti and agouti-related protein: analogies and contrast. *J Biol Chem* 275:6695–6698
 10. Lu D, Willard D, Patel IR, Kadwell S, Overton L, Kost T, Luhter M, Chen W, Woychik RP, Wilkinson WO 1994 Agouti protein is an antagonist of the melanocyte-stimulating-hormone receptor. *Nature* 371:799–802
 11. Ollmann MM, Wilson BD, Yang YK, Kerns JA, Chen I, Gantz I, Barsh GS 1997 Antagonism of central melanocortin receptors *in vitro* and *in vivo* by agouti-related protein. *Science* 278:135–138
 12. Chen AS, Marsh DJ, Trumbauer ME, Frazier EG, Guan XM, Yu H, Roseblum CI, Vongs A, Feng Y, Cao L, Metzger JM, Strack AM, Camacho RE, Mellin TN, Nunes CN, Min W, Fisher J, Gopal-Truter S, MacIntyre DE, Chen HY, Van der Ploeg LH 2000 Inactivation of the mouse melanocortin-3 receptor results in increased fat mass and reduced lean body mass. *Nat Genet* 26:97–102
 13. Huszar D, Lynch CA, Fairchild-Huntress V, Dunmore JH, Fang Q, Berke-meier LR, Gu W, Kesterson RA, Boston BA, Cone RD, Smith FJ, Campfield LA, Burn P, Lee F 1997 Targeted disruption of melanocortin-4 receptor results in obesity in mice. *Cell* 88:131–141
 14. Klebig ML, Wilkinson JE, Geisler JG, Woychik RP 1995 Ectopic expression of the agouti gene causes obesity, features of type II diabetes, and yellow fur. *Proc Natl Acad Sci USA* 92:4728–4732
 15. Kucera GT, Bortner DM, Rosenber MP 1996 Overexpression of an agouti cDNA in the skin of transgenic mice recapitulates dominant coat color phenotypes of spontaneous mutants. *Dev Biol* 173:162–173
 16. Rossi M, Kim MS, Morgan DGA, Small CJ, Edwards CMB, Sunter D, Abusana S, Goldstone AP, Russel SH, Stanley SA, Smith DM, Yagaloff K, Ghatei MA, Bloom SR 1998 A C-terminal fragment of agouti-related protein increases feeding and antagonizes the effect of alpha-melanocyte stimulating hormone *in vivo*. *Endocrinology* 139:4428–4431
 17. Fan W, Boston BA, Kesterson RA, Hruby VJ, Cone RD 1997 Role of melanocortinergic neurons in feeding and the agouti obesity syndrome. *Nature* 385:165–168
 18. Kask A, Mutulis R, Muceniec R, Pahkla R, Mutule I, Wikberg JE, Rago L, Schiöth HB 1998 Discovery of a novel superpotent and selective melanocortin-4 receptor antagonist (HS024): evaluation *in vitro* and *in vivo*. *Endocrinology* 139:5006–5014
 19. Marsh DJ, Holloper G, Huszar D, Laufer R, Yagaloff KA, Fisher SL, Burn P, Palmiter RD 1999 Response of melanocortin-4 receptor-deficient mice to anorectic and orexigenic peptides. *Nature* 21:119–122
 20. Lin X, Volkoff H, Narnaware Y, Bernier NJ, Peyon P, Peter RE 2000 Brain regulation of feeding behavior and food intake in fish. *Comp Biochem Physiol* 126A:415–434
 21. Ringholm A, Fredriksson R, Poliakov N, Yan YL, Postlethwait JH, Larhammar D, Schiöth HB 2002 One melanocortin 4 and two melanocortin 5 receptors from zebrafish show remarkable conservation in structure and pharmacology. *J Neurochem* 82:6–18
 22. Wilson MR, Middleton D, Warr GW 1991 Immunoglobulin V_H genes of the goldfish, *Carassius auratus*: a re-examination. *Mol Immunol* 28:449–457
 23. Horn F, Vriend G, Cohen FE 2001 Collecting and harvesting biological data: the GPCRDB, NucleaRDB information systems. *Nucleic Acids Res* 29:346–349
 24. Marklund U, Bystrom M, Gedda K, Larefalk A, Juneblad K, Nystrom S, Ekstrand AJ 2002 Intron-mediated expression of the human neuropeptide Y Y1 receptor. *Mol Cell Endocrinol* 188:85–97
 25. Nordstedt C, Fredholm BB 1990 A modification of a protein-binding method for rapid quantification of cAMP in cell-culture supernatants and body fluid. *Anal Chem* 189:231–234
 26. Peyon P, Lin XW, Himick BA, Peter RE 1998 Molecular cloning and expression of cDNA encoding brain preprocholecystokinin in goldfish. *Peptides* 19:199–210
 27. Cerdá-Reverter JM, Martínez-Rodríguez G, Anglade I, Kah O, Zanuy S 2000 Peptide YY (PYY) and fish pancreatic peptide Y (PY) expression in the brain of the sea bass (*Dicentrarchus labrax*) as revealed by *in situ* hybridization. *J Comp Neurol* 426:197–208
 28. Peter RE, Gill VE 1975 A stereotaxical atlas and technique for forebrain nuclei of the goldfish, *Carassius auratus*. *J Comp Neurol* 159:69–101
 29. Bernier NJ, Peter RE 2001 Appetite-suppressing effects of urotensin I and corticotrophin-releasing hormone in goldfish (*Carassius auratus*). *Neuroendocrinology* 73:248–260
 30. Cerdá-Reverter JM, Zanuy S, Munoz-Cueto JA 2001 Cytoarchitectonic study of the brain of a perciform species, the sea bass (*Dicentrarchus labrax*). II. The diencephalon. *J Morphol* 247:229–251
 31. Schiöth HB, Petersson S, Muceniec R, Szardenings M, Wikberg JE 1997 Deletions of the N-terminal regions of the human melanocortin receptors. *FEBS Lett* 410:223–228
 32. Yang Y, Dickinson C, Haskell-Luevano C, Gantz I 1997 Molecular basis for the interaction of [Nle⁴, D-Phe⁷] melanocyte stimulating hormone with the human melanocortin-1 receptor. *J Biol Chem* 272:23000–23010
 33. Takahashi A, Amemiya Y, Nozaki M, Sower SA, Kawachi H 2001 Evolutionary significance of proopiomelanocortin in agnatha and chondrichthyes. *Comp Biochem Physiol* 129B:283–289
 34. Takeuchi S, Takahashi S 1998 Melanocortin receptors genes in the chicken—tissue distribution. *Gen Comp Endocrinol* 112:220–231
 35. Teshigawara K, Takahashi S, Boswell T, Li Q, Tanaka S, Takeuchi S 2001 Identification of avian alpha-melanocyte-stimulating hormone in the eye: temporal and spatial regulation of expression in the developing chicken. *J Endocrinol* 168:527–537
 36. Oliverau M, Oliveureau JM 1990 Corticotropin-like immunoreactivity in the brain and pituitary of three teleost species (goldfish, trout and eel). *Cell Tiss Res* 262:115–123
 37. Mountjoy KG, Mortrud MT, Low MJ, Simerly RB, Cone RD 1994 Localization of the melanocortin-4 receptor (MC4-R) in neuroendocrine and autonomic control circuits in the brain. *Mol Endocrinol* 810:1298–1308
 38. Kishi T, Aschkenasi CJ, Lee CE, Mountjoy KG, Saper CB, Elmquist JK 2003 Expression of melanocortin 4 receptor mRNA in the central nervous system of rat. *J Comp Neurol* 457:213–235
 39. Norcutt RG 1995 The forebrain of gnathostomes: in search of a morphotype. *Brain Behav Evol* 46:275–318
 40. Braford Jr MR 1995 Comparative aspects of forebrain organization in the ray-finned fishes: touchstones or not? *Brain Behav Evol* 46:259–274
 41. Kah O, Anglade I, Lepretre E, Doboug P, de Monbrison D 1993 The reproductive fish brain. *Fish Physiol Biochem* 11:85–98
 42. Peng C, Gallin W, Peter RE, Blomqvist AG, Larhammar D 1994 Neuropeptide Y gene expression in the goldfish brain: distribution and regulation by ovarian steroids. *Endocrinology* 134:1095–1103
 43. Peng C, Chang JP, Yu KL, Wong AO-L, Van Goor F, Peter RE, Rivier JE 1993 Neuropeptide Y stimulates growth hormone and gonadotropin-II secretion in the goldfish pituitary: involvement of both presynaptic and pituitary cell actions. *Endocrinology* 132:1820–1829
 44. Rao SD, Rao PD, Peter RE 1996 Growth hormone-releasing hormone immunoreactivity in the brain, pituitary, and pineal of the goldfish, *Carassius auratus*. *Gen Comp Endocrinol* 102:210–220
 45. Oliveureau M, Ollevier F, Vandesande F, Verdonck W 1984 Immunocytochemical identification of CRF-like and SRIF-like peptides in the brain and the pituitary of cyprinid fish. *Cell Tiss Res* 237:379–382
 46. Wendelaar Bonga SE 1997 The stress response in fish. *Physiol Rev* 77:591–625
 47. Peter RE 1979 The brain and feeding behavior. In: Hoar WS, Randall DJ, Brett JR, eds. *Fish physiology*. New York: Academic Press; 121–159, vol VIII
 48. Demski LS, Knigge KM 1971 The telencephalon and hypothalamus of bluegill (*Lepomis macrochirus*): evoked feeding, aggressive and reproductive behavior with representative frontal sections. *J Comp Neurol* 143:1–16
 49. Rink E, Wulliman MF 1998 Some forebrain connection of the gustatory system in the goldfish *Carassius auratus* visualized by separate DiI application to the hypothalamic inferior lobe and the torus lateralis. *J Comp Neurol* 394:152–170
 50. Narnaware YK, Peter RE 2001 Effects of food deprivation and refeeding on neuropeptide Y (NPY) mRNA levels in goldfish. *Comp Biochem Physiol* 129B:633–637
 51. Silverstein J, Breining J, Baskin DG, Plisetskaya EM 1998 Neuropeptide Y-like gene expression in the salmon brain increases with fasting. *Gen Comp Endocrinol* 110:157–165
 52. Narnaware YK, Peyon PP, Lin X, Peter RE 2000 Regulation of food intake by neuropeptide Y in goldfish. *Am J Physiol* 279:R1025–R1034
 53. Schiöth HB, Bouifrouri AA, Rudzish R, Muceniec R, Watanobe H, Wikberg JE, Larhammar D 2002 Pharmacological comparison of rat and human melanocortin 3 and 4 receptors *in vitro*. *Regul Pept* 106:7–12
 54. Yada T, Moriyama S, Suzuki Y, Azuma T, Takahashi A, Hirose S, Naito N 2002 Relationship between obesity and metabolic hormones in the “cobalt” variant of rainbow trout. *Gen Comp Endocrinol* 128:36–43
 55. Gantz I, Miwa H, Konda Y, Shimoto Y, Tashiro T, Watson SJ, DelValle J, Yamada T 1993 Molecular cloning, expression, and gene localization of a fourth melanocortin receptor. *J Biol Chem* 268:15174–15179
 56. Chhajlani V, Muceniec R, Wikberg JES 1993 Molecular cloning of a novel human melanocortin receptor. *Biochem Biophys Res Commun* 195:866–873
 57. Alvaro JD, Tatro JB, Quillan JM, Fogliano M, Eisenhard M, Lerner MR, Nestler EJ, Duman RS 1996 Morphine down-regulates melanocortin-4 receptor expression in brain regions that mediate opiate addiction. *Mol Pharmacol* 50:583–591
 58. Griffon N, Mignon V, Facchinetti P, Diaz J, Schwartz JC, Sokoloff P 1994 Molecular cloning and characterization of the rat fifth melanocortin receptor. *Biochem Biophys Res Commun* 200:1007–1014
 59. Schiöth HB, Mutulis F, Muceniec R, Prusis P, Wikberg JES 1998 Discovery of novel melanocortin 4 receptor selective MSH analogues. *Br J Pharmacol* 124:75–82